**A MORPHOLOGICAL EVALUATION OF CRATER DEGRADATION ON MERCURY: REVISITING CRATER CLASSIFICATION WITH MESSENGER DATA.** Mallory J. Kinczyk[1], Louise M. Prockter[1], Clark R. Chapman[2], and Hannah C. M. Susorney[3]. [1]The Johns Hopkins University Applied Physics Laboratory, Laurel, MD 20723 USA (mallory.kinczyk@jhuapl.edu). [2]Department of Space Studies, Southwest Research Institute, Boulder, CO 80302 USA. [3]Department of Earth and Planetary Sciences, The Johns Hopkins University, Baltimore, MD 21218 USA.

**Introduction:** The application of crater degradation as a tool for the relative age dating of geological units has been an important component in deriving interplanetary correlations of geologic time [1]. First developed for the Moon [e.g., 2-4], the degradation classification system was later extrapolated to Mercury [1,5]. Though these initial studies used a 4- or 5-class system ranging from fresh to very degraded, there have been several classification systems used since, and morphological variations exist among them. The first quadrangle maps of Mercury, derived from Mariner 10 image data, applied a later-developed 5-class system, in which the base of each class corresponds to an approximate age (Pre-Tolstojan, older than ~4.0 Gyr; Tolstojan, ~3.9–4.0 Gyr; Calorian, ~3.9 Gyr; Mansurian, ~3.0–3.5 Gyr; and Kuiperian, ~1 Gyr) [6]. However, different quadrangle mappers applied different descriptions and interpretations of the crater morphology in each class, making it challenging to reliably compare and interpret the maps.

The global image dataset acquired by the Mercury Dual Imaging System (MDIS) on the MErcury, Surface, Space, ENvironment, GEochemistry, and Ranging (MESSENGER) spacecraft allows for rigorous classification of craters previously imaged by Mariner 10, as well as the classification of craters in newly imaged regions of Mercury. In this study, we attempt to standardize classification for Mercurian craters by developing a consistent scheme based on clear, uniform morphological criteria. We classified all Mercurian craters ≥40 kilometers in diameter with our system, thus establishing the first global dataset of crater degradation on Mercury and providing a useful tool for understanding the evolution of Mercury's surface.

**Data and Methods:** We classified craters from a global database of large impact craters ≥ 20 km in diameter [7] on the basis of their degree of morphological degradation. Six MDIS monochrome and color global image mosaics [8], each with different viewing geometries, were used to find the ideal lighting and resolution conditions to view crater morphology and identify ray systems. Topographic data derived from stereo imaging [9] aided in the identification of texture and crater ejecta.

Our classification scheme, where Class 1 is fresh and Class 5 is very degraded, is an updated approach that still maintains the chronological relationships established earlier [1]. From a comprehensive evaluation of previous class descriptions for Mercurian craters [1,6], we identified the most important diagnostic morphological features for each class. These include rays, rim freshness, wall terracing, ejecta facies, central peak features, and the presence and abundance of interior smooth plains. A matrix (not shown) was derived from previous interpretations of the classification scheme to segregate the primary individual morphological characteristics by degradation class. Because of a higher relative rate of degradation of smaller craters [5], a second matrix (Figure 1) was developed to display incremental crater degradation over all mapped initial crater sizes and morphologies [10,11].

High-incidence angle images and low image resolution make accurate and consistent crater classification difficult for some portions of Mercury's surface. Image resolution limitations also make the identification of morphological features challenging at smaller diameters. Craters <40 km in diameter were not classified for this reason. Additionally, crater morphology can be markedly changed by the later formation of a large crater nearby [1,6]. As this proximity-weathering process can cause craters to appear older than they are, craters close to major stratigraphic markers (e.g., the Caloris basin) have been classified with a higher level of confidence because relative age relationships are more easily identified (e.g., a heavily degraded crater that superposes Caloris ejecta must be of Calorian age – Class 3 – or younger).

**Discussion:** There is a lack of mid-size Class 5 (Pre-Tolstojan) craters between 0° and 90°E in contrast to the more random distributions of the other four classes of craters. The region between 0° and 90°E is dominated by intercrater plains with few patches of smooth plains, insufficient to suggest abundant volcanic resurfacing as a cause. Unconfirmed basins b30 (1390 km diameter) and b56 (~1000–1500 km diameter) [11] have been classified as Pre-Tolstojan in age and are located in this region. These basins are sufficiently large to have obliterated a large number of mid-size craters, possibly contributing to this pattern.

Size-frequency distributions (Figure 2) indicate that for Classes 4 through 2 and diameters ranging from 50 to 200 km, the ratio of craters in each class remains relatively constant, suggesting that craters spend equal percentages of their lifetimes transitioning through each degradational class, independent of size or rapidity of their degradation. The slightly larger percentages of Class 4 craters >200 km in diameter and the substantially larger percentages of Class 5 craters than Class 4 craters at diameters >500 km suggest that

additional processes degrade the largest craters and basins (e.g., shallower initial depth/diameter ratios, potential topographic relaxation of large features, and/or widespread volcanism). A more in-depth study will be necessary to better understand how these processes have contributed to the distribution of craters in each class.

**References:** [1] McCauley, J. F. et al. (1981). *Icarus, 47,* 184–202. [2] Arthur, D. W. G. et al. (1963) *Comm. LPL, 2, #30,* 71–78. [3] Trask, N. J. (1967) *Icarus, 6,* 270–276. [4] Chapman, C. R. (1968) *Icarus, 8,* 1–22. [5] Wood, C. A. et al. (1977) *LPS, 8,* 3503 –3520. [6] Spudis, P. D. and Guest, J. E. (1988). In *Mercury*, Univ. Arizona Press, pp. 118–164. [7] Fassett, C. I. et al. (2011). *Geophys. Res. Lett., 38,* 1–6. [8] Chabot, N. L. et. al. (2016) *LPS, 47,* #1256. [9] Gaskell, R. W. et al. (2011). *AGU,* P41A-1576. [10] Pike, R. J. (1988). In *Mercury*, Univ. Arizona Press, pp. 165–273. [11] Baker, D. M. H. et al. (2011). *Planet. Space Sci., 59,* 1932–1948.

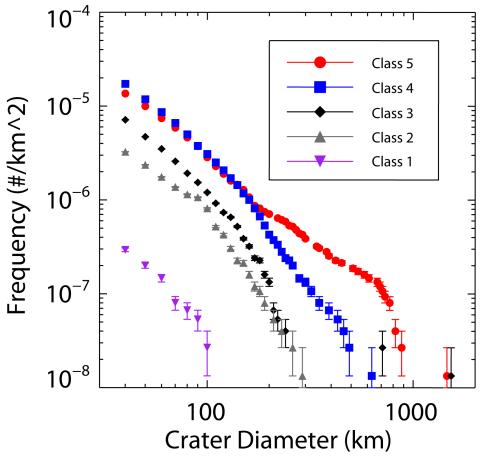


**Figure 2.** Cumulative size-frequency distribution of classified craters >40 km in diameter on Mercury's surface.

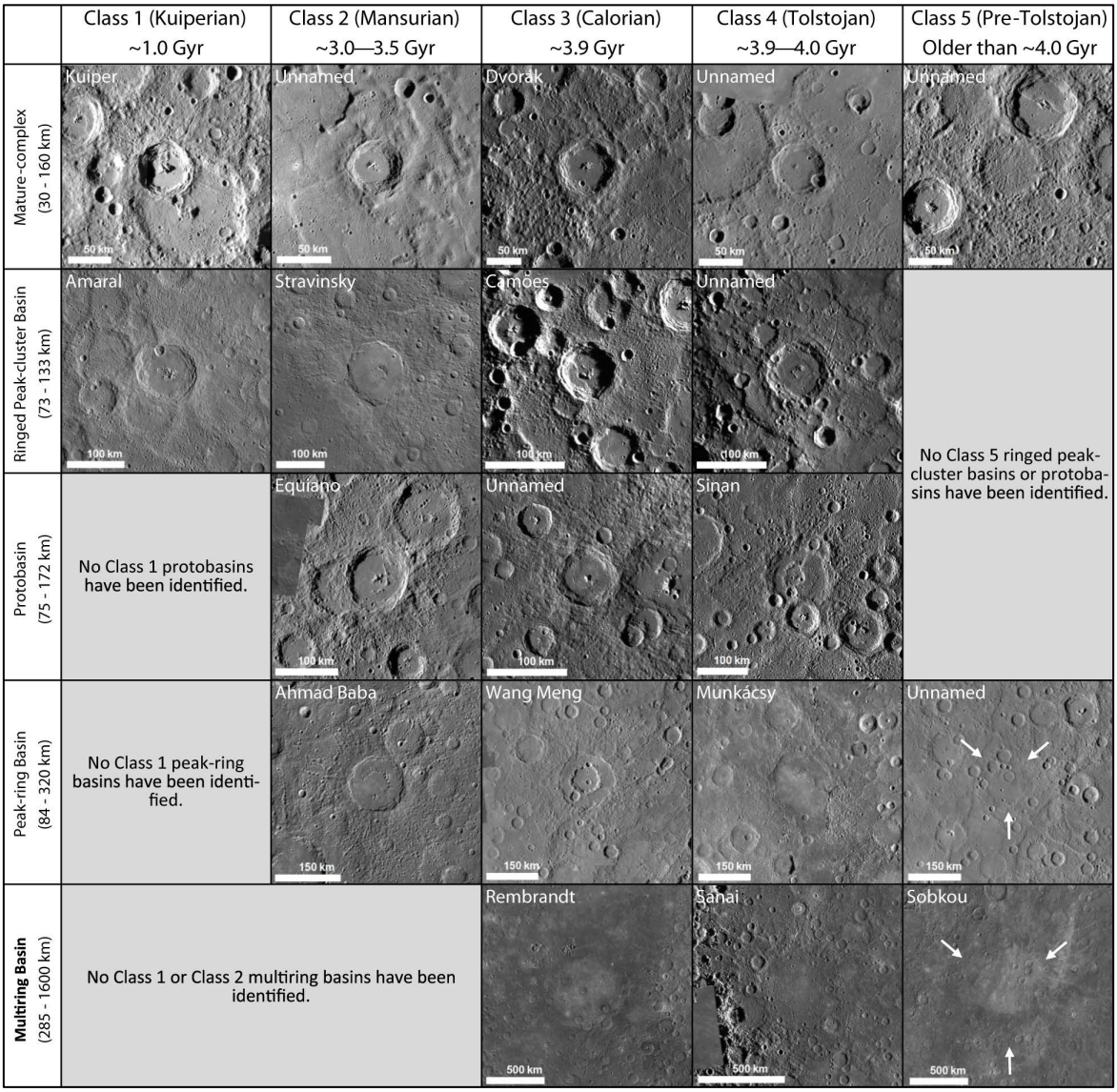


**Figure 1.** Craters of each morphological type [10,11] are broken down into classes of degradation. Ages are derived from previous models [6] and indicate the base of each system. Selected craters are centered in each image with diameters approximately one third the width of the image.